

## Radiation absorbed by a vertical cylinder in complex outdoor environments under clear sky conditions

S.A. Kryś and R.D. Brown

School of Landscape Architecture, University of Guelph, Guelph, Ontario, Canada N1G 2W1

Received May 22, 1989; revised December 7, 1989

Accepted December 21, 1989

**Abstract.** Research was conducted into the estimation of radiation absorbed by a vertical cylinder in complex outdoor environments under clear sky conditions. Two methods of estimation were employed: a cylindrical radiation thermometer (CRT) and model developed by Brown and Gillespie (1986), and the weather station model. The CRT produced an integrated temperature reading from which the radiant environment could be estimated successfully given simultaneous measurements of air temperature and wind speed. The CRT estimates compared to the measured radiation gave a correlation coefficient of 0.9499,  $SE = 19.8 \text{ W/m}^2$ ,  $\alpha = 99.9\%$ . The physically-based equations (weather station model) require the inputs of data from a nearby weather station and site characteristics to estimate radiation absorbed by a vertical cylinder. The correlation coefficient for the weather station model is 0.9529,  $SE = 16.8 \text{ W/m}^2$ ,  $\alpha = 99.9\%$ . This model estimates short wave and long wave radiation separately; hence, this allowed further comparison to measured values. The short wave radiation was very successfully estimated:  $R = 0.9865$ ,  $SE = 10.0 \text{ W/m}^2$ ,  $\alpha = 99.9\%$ . The long wave radiation estimates were also successful:  $R = 0.8654$ ,  $SE = 15.7 \text{ W/m}^2$ , and  $\alpha = 99.9\%$ . Though the correlation coefficient and standard error may suggest inaccuracy to the micrometeorologist, these estimation techniques would be extremely useful as predictors of human thermal comfort which is not a precise measure but defined by a range. The reported methods require little specialized knowledge of micrometeorology and are vehicles for the designers of outdoor spaces to measure accurately the inherent radiant environment of outdoor spaces and provide a measurement technique to simulate or model the effect of various landscape elements on planned environments.

**Key words:** Human thermal comfort – Radiation (absorbed) – Outdoor microclimates – Human energy budget – Microclimate simulation

### Introduction

Designers of outdoor spaces require methods to discern micrometeorological conditions quickly and easily, to recognize and map the inherent micrometeorological properties of a site, and to evaluate and enhance human thermal comfort (HTC) of a site during the design process. To use HTC models, designers need to estimate accurately several micrometeorological parameters. One of the very complex and important inputs is the radiation received from the sun and surrounding environment.

In this paper two approaches to solving this problem are tested. First, a cylindrical radiation thermometer (CRT) and associated model developed by Brown and Gillespie (1986) is tested for its ability to measure net radiation load on a vertical cylinder in complex outdoor environments. The second model tested (Brown 1985) is a set of equations based on meteorological physics. This model uses weather station data and the physical parameters of a remote site to estimate radiation absorbed by a vertical cylinder at that site. Clear sky conditions were chosen for this first examination to limit the variables.

A vertical cylinder is the common denominator in these tests, being generally accepted as the geometric shape that best mimics a standing person (e.g. Campbell 1977). The resulting data from both tests can go directly into the HTC model developed by Brown and Gillespie (1986). The degree of accuracy required of the CRT and weather station (WS) model is somewhat less than a micrometeorologist demands, as human thermal comfort is expressed as a range rather than a single value. Designers are looking for comparative values to define spaces of greater or lesser radiation loads, and to understand how landscape elements affect both short and long wave radiation loads so the manipulation of elements can more effectively enhance HTC.

### Materials and methods

The ten outdoor sites chosen for this study represented a range of sun/shade conditions: six sites were in the shade of single trees

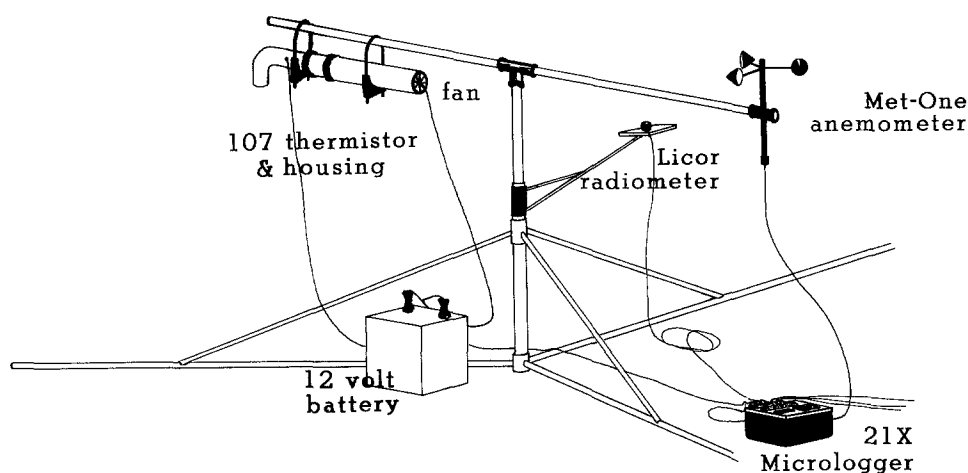


Fig. 1. Weather station instruments

of various species (*Salix alba tristis*, *Picea glauca*, *Catalpa speciosa*, *Thuja occidentalis*, *Acer negundo*, *Acer saccharinum*), three sites were open flat grassy fields, and one was in the shade of a building. The *S. alba tristis*, *P. glauca* and one open field site were measured in two different seasons, spring and fall. The ground cover in all locations was grass. All sites were in Guelph, Ontario, Canada (latitude  $43^{\circ}43'$ , longitude  $80^{\circ}17'$ ) within a 200 m radius. Measurements were taken on April 9 and 10, 1988 and September 29, 1989. The sky was completely cloudless for the duration of all measurements.

The equipment was assembled as two units: weather station instruments and mobile instruments. The weather station instruments were assembled on a sturdy tripod with extensions to hold each of three instruments; a radiometer (Li-cor, Lincoln, Neb.), an anemometer (Met-One, Campbell Scientific, Logan, Utah) and a 107 thermistor (Campbell Scientific) in a ventilated radiation shield. All instruments were newly levelled or plumbed at each test site. The extension supporting the Li-cor radiometer was always oriented directly toward the sun to prevent error due to shading. The anemometer was set 1.5 m above the ground. Figure 1 shows the configuration of the weather station instruments.

The mobile instruments consisted of a pyrgeometer (Eppley, EPLAB, Newport, RI, USA), a radiometer (Eppley pyrhelometer, EPLAB) and a cylindrical radiation thermometer (Brown and Gillespie 1986) modified to allow electronic recording. The Eppley radiometer and pyrgeometer were mounted on a square platform so the effective sensing surfaces were level and planar. The CRT was mounted 400 mm from the other instruments, in such a way as to be vertical when the platform was tipped  $90^{\circ}$ . The platform was then fitted to a sturdy tripod with a fully articulating deck. The deck allowed the platform to be tipped  $90^{\circ}$  and rotated  $360^{\circ}$  to any directional orientation. Figure 2 illustrates the assembly of the mobile instruments.

The CRT, as described by Brown and Gillespie (1986) has been modified for electronic monitoring. The modified CRT is an aluminum cylinder 106.44 mm in length and 9.81 mm in diameter with a hole 6 mm in diameter drilled 42.72 mm deep to fit a 107 thermistor (Campbell Scientific). The painted surface of the cylinder has an albedo of 0.37 and an emissivity of 0.95 (Brown and Gillespie 1986). The CRT was mounted on a laminated plexiglas strip of dimensions 600 mm  $\times$  15 mm  $\times$  15 mm. The strip was attached to one edge of the square Eppley platform leaving a 400 mm extension. On the cantilevered end of the strip a hole of 9.82 mm in diameter was drilled 10 mm down and perpendicular to the plexiglas surface. A second hole of 7.5 mm in diameter was drilled on centre through the remaining 5 mm of plexiglas. The CRT was inserted into the larger hole and seated perpendicular to the plexiglas surface. A 107 thermistor was coated with "Thermal Compound" (Wakefield Engineering) and inserted through

the smaller hole to a depth of 42.72 mm into the aluminum cylinder. The 107 thermistor was wired and programmed into the Micrologger. Figure 3 illustrates the CRT and the plexiglas mount in longitudinal cross-section.

The energy budget for the cylinder, provided by Brown and Gillespie (1986) is calculated in the following manner:

$$R_{abs} = \sigma (T_{crt} + 273.15)^4 + (lC_p) (T_{crt} - T_{air})/r_m$$

where:

$\sigma$  = the Stefan-Boltzmann constant ( $5.67 \times 10^{-8} \text{ W m}^{-2} \text{ K}^{-4}$ )

$lC_p$  = volumetric heat capacity of air ( $\sim 1200 \text{ J m}^{-3} \text{ K}^{-1}$ )

$T_{crt}$  = equilibrium temperature of CRT ( $^{\circ}\text{C}$ ), and

$T_{air}$  = temperature of the air ( $^{\circ}\text{C}$ ).

Brown and Gillespie (1986) have modelled resistance  $r_m$  using the following expression:

$$r_m = D / (A Re^n Pr^{0.33} k)$$

where:

$Re$  = Reynolds number  $= V_{\infty} D / \nu$

$Pr$  = Prandtl number  $\sim 0.71$

$D$  = diameter of a cylinder

$V_{\infty}$  = free stream air velocity

$\nu$  = kinematic viscosity

$k$  = thermal diffusivity of the air

and  $A$  and  $n$  are empirical constants derived through experiments on heat flow from cylinders (Kreith and Black 1980; Equation 5-26 and Table 5-2).

All instruments were connected to a 21X Micrologger (Campbell Scientific) and programmed to record integrated readings at 1-min intervals. At each test site, the Eppleys were oriented horizontally and placed in full sun next to the weather station assembly to allow for calibration of the radiometers. To model radiation incident on a vertical cylinder, the Eppleys were moved into the test location, tipped  $90^{\circ}$  to measure radiation incident on four vertical planes oriented directly towards the sun, directly away from the sun and in the two directions normal to this axis. A similar approach was used by de Freitas (1985). The normalized average beam radiation was then divided by  $\pi$  to determine  $\text{W/m}^2$ .

The first location tested was in the shade of a willow. The tripods were set side by side in full sun to calibrate the radiometers, and the instruments were then moved under the leafless boughs of the willow. The willow had a drooping form with some branches trimmed to less than 1 m above the ground. The centre of the platform was measured 1.3 m above the ground. The tripod was placed 3 m north-northeast of the tree trunk. The Eppleys were tipped  $90^{\circ}$  so the effective sensing surfaces of the instruments

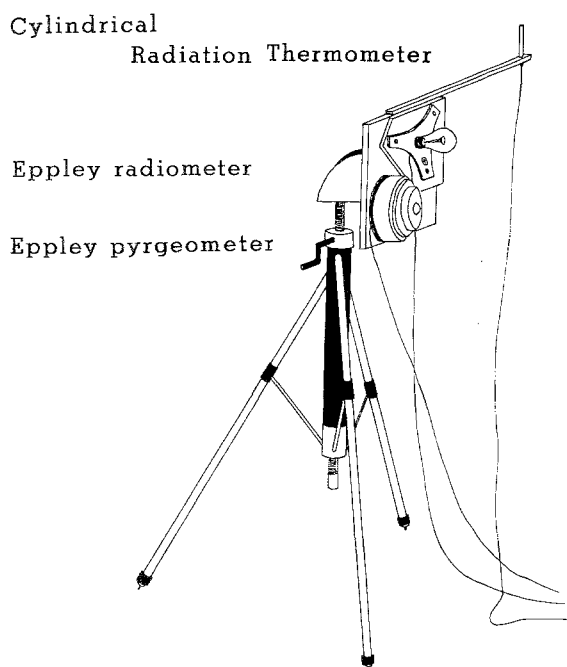


Fig. 2. Mobile instruments

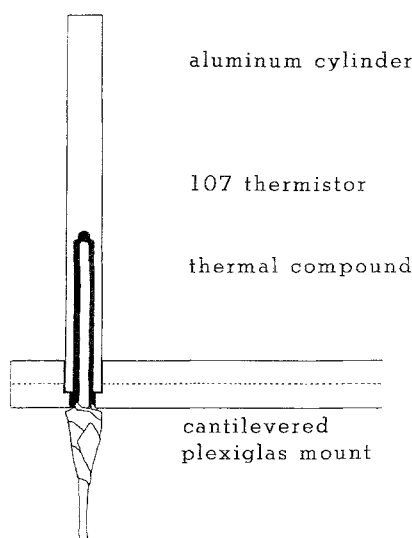


Fig. 3. Cross-section of CRT and mount

were vertical, plumb and allowed to record two 1-minute readings in each directional orientation. In each case the reading with the highest wind speed was used, as the anemometer had a stall speed of 0.5 m/s which was to be avoided. Measurements were taken on April 9, 1988 between 1049 h and 1127 h Eastern Daylight Time (EDT). Each test location was measured in the same manner. Table 1 lists all test locations and the date and time measurements were taken.

## Results and analysis

This paper sets out the investigation of two proposals: to test a new instrument (CRT) and model for accuracy in determining the radiation absorbed by a vertical cylinder and to test a physically based model that uses only

Table 1. Test site locations

Location		Date	Time
<i>Acer negundo</i>	Manitoba maple	29 Sept 89	1428 h–1436 h
<i>Acer saccharinum</i>	Silver maple	29 Sept 89	1451 h–1503 h
<i>Catalpa speciosa</i>	Catalpa	29 Sept 89	1230 h–1242 h
<i>Salix alba tristis</i>	Weeping willow		
	willow 1	09 April 88	1049 h–1127 h
	willow 2	29 Sept 89	1323 h–1336 h
<i>Picea glauca</i>	White spruce		
	spruce 1	09 April 88	1147 h–1222 h
	spruce 2	29 Sept 89	1253 h–1311 h
<i>Thuja occidentalis</i>	White cedar	29 Sept 89	1403 h–1416 h
Open field 1		09 April 88	1246 h–1319 h
Open field 2		29 Sept 89	1210 h–1221 h
Open field 3		29 Sept 89	1507 h–1537 h
Building		10 April 88	1434 h–1543 h

weather station data and site parameters for estimating radiation absorbed by a cylinder. The results of each test were compared to the measured radiation absorbed. The radiometers used to measure short and long wave radiation required mathematical interpretation to produce a reading of radiation absorbed by a vertical cylinder. Measurements in each location were done over a period of time – between 0.25 and 1.25 h at each site – therefore it was necessary to normalize measured values of each site to a median time to emulate simultaneous measurements from all directions and eliminate error due to changing solar elevation.

Short wave radiation were calculated as an average of short wave radiation down ( $K\downarrow$ ) using four orientations: directly into the sun, directly away from the sun and the two directions normal to the axis. Long wave radiation down ( $L\downarrow$ ) was also averaged to simulate all directional measurements being made simultaneously. The  $L\downarrow$  used for comparison in this paper was calculated from the values of four directional orientations

Table 2. Measured and calculated absorbed radiation values by a vertical cylinder at test locations ( $W/m^2$ )

Location	$K\downarrow$	$K_{abs}$	$L\downarrow$	$L_{abs}$	$R_{abs}$
Manitoba maple	86	54	408	388	442
Silver maple	91	57	408	388	445
Catalpa	89	57	414	393	449
Spruce 1	74	47	309	294	341
Spruce 2	68	43	408	388	431
Willow 1	181	114	307	292	406
Willow 2	73	46	408	388	434
Cedar	81	51	408	388	439
Open field 1	323	203	340	323	526
Open field 2	272	171	370	352	523
Open field 3	344	217	407	387	604
Building	63	40	353	335	375

of the Eppley pyrgeometer: directly into the sun, directly away from the sun and the two directions normal to the axis. The proportion of radiation absorbed by a cylinder must then be calculated from these averages. The  $K\downarrow$  was adjusted to account for the albedo of the cylinder for short wave absorbed ( $K_{abs}$ ) and  $L\downarrow$  was adjusted for the emissivity factor of the cylinder for long wave radiation absorbed ( $L_{abs}$ ). The short and long wave radiation absorbed by the cylinder are totalled for radiation absorbed ( $R_{abs}$ ). These values are summarized in Table 2.

The CRT reading is an integration of inputs and outputs of radiation on a vertical cylinder, therefore proportions of short and long wave radiation are indistinguishable. The measured readings from the radiometers were an amalgamation of readings over time, therefore the CRT values were averaged to maintain consistency. The instrument is designed to be accurate with only one reading; however care must be taken to allow the instrument to reach equilibrium before recording the reading. Table 3 displays the estimated radiation absorbed ( $R_{abs}$ ) by a vertical cylinder made with the CRT and measurements of air temperature and wind speed from the weather station necessary for the model.

**Table 3.** Estimated radiation absorbed using the cylindrical radiation thermometer ( $W/m^2$ )

Location	Air temperature	Wind speed	Temperature of CRT	Estimated radiation absorbed by a cylinder
	$T_{air}$	$\bar{U}$	$T_{crt}$	
Manitoba maple	18.25	3.43	19.40	463
Silver maple	18.26	3.39	19.28	457
Catalpa	18.50	3.25	19.30	446
Spruce 1	6.59	2.30	7.36	374
Spruce 2	18.25	3.10	19.04	443
Willow 1	4.77	1.94	7.18	414
Willow 2	18.32	3.33	19.04	442
Cedar	18.26	4.35	19.20	461
Open field 1	8.86	1.39	13.37	473
Open field 2	18.50	2.67	22.00	550
Open field 3	17.44	3.47	21.35	592
Building	14.95	2.08	15.11	395

The third task was to test for the ability of the physically based model to estimate the radiation absorbed by a cylinder using weather station data and estimates of site characteristics. The inputs necessary for the physically based mathematical model and how the estimates/measurements were attained are listed below:

- 1) solar elevation – calculated from time of day, time of solar noon, declination and latitude;
- 2) air temperature measurement – from weather station;
- 3) wind speed measurement – from weather station;
- 4) estimated albedo of the objects in the sky and ground hemispheres – from the literature, whenever available;
- 5) estimated temperature of objects in the sky and

ground hemispheres – from the literature, whenever available;

6) estimated sky view factor – roughly estimated from photographs; and

7) estimated percentage of full sun in the test environment – roughly estimated on-site and from photographs.

The values used at each test location are included in Appendix I.

The equations of the weather station model are given in Appendix II: willow 1 inputs are used in example. The model calculates short and long wave radiation separately which allows more relevant comparisons. Table 4 lists the  $K_{abs}$ ,  $L_{abs}$  and  $R_{abs}$  as estimated by the weather station model at each test location.

**Table 4.** Estimated radiation absorbed by a vertical cylinder using weather station model ( $W/m^2$ )

Location	$K_{abs}$	$L_{abs}$	$R_{abs}$
Manitoba maple	65	380	445
Silver maple	63	364	427
Catalpa	72	369	441
Spruce 1	71	303	374
Spruce 2	67	364	431
Willow 1	120	310	430
Willow 2	59	384	443
Cedar	64	364	428
Open field 1	178	296	474
Open field 2	176	359	535
Open field 3	213	343	556
Building	36	349	385

Table 5 summarizes  $R_{abs}$  from the two tests against the measured values. Both methods estimated  $R_{abs}$  to within 10% of the measured value.

**Table 5.** Measured radiation compared to estimated radiation using CRT and weather station model ( $W/m^2$ )

Location	Measured $R_{abs}$ of a cylinder	Estimation radiation	
		CRT	weather station model
Manitoba maple	442	463	445
Silver maple	445	457	427
Catalpa	450	446	441
Spruce 1	341	374	374
Spruce 2	431	443	431
Willow 1	406	414	430
Willow 2	434	442	443
Cedar	439	461	428
Open field 1	526	473	474
Open field 2	523	550	535
Open field 3	604	592	556
Building	375	395	385

As the weather station model distinguishes between short and long wave radiation, it is also possible to test for some precision of the model. Table 6 lists the measured and estimated long and short wave values.

The weather station model consistently overestimates the short wave radiation in all conditions of tree shade.

**Table 6.** Measured short and long wave radiation values compared to those estimated with the weather station model ( $\text{W/m}^2$ )

Location	$K_{abs}$		$L_{abs}$	
	Measured	WS	Measured	WS
Manitoba maple	54	65	388	380
Silver maple	57	63	388	364
Catalpa	57	72	393	369
Spruce 1	47	71	294	303
Spruce 2	43	67	388	364
Willow 1	114	120	292	310
Willow 2	46	59	388	384
Cedar	51	64	388	364
Open field 1	203	178	323	296
Open field 2	171	176	352	359
Open field 3	217	213	387	343
Building	40	36	335	350

Possibly this is a reflection of unrefined techniques of estimating sky view factor and transmissivity. The open field situations are more normally distributed, the under-estimate in the open field 1 situation is possibly the result from a poor estimate of percent diffuse transmissivity. In all three cases, long wave radiation is under-estimated by the weather station model. In all but two cases, the error in short wave is ameliorated by the error in long wave; hence,  $R_{abs}$  (WS) reflect a very accurate estimate that could be more precise.

Each of the input variables for this model was subjected to a sensitivity test to determine the precision required in estimating that variable. Sensitivity was determined by the change in each variable input required to produce a  $\pm 10\%$  change in  $R_{abs}$ . This information is summarized in Appendix III. The most influential variable in the model is solar elevation: the input would require a minimum 2% error to create a 1% change in  $R_{abs}$ . Calculation of solar elevation could be included in the model if this is a common source of error in application. No single variable has great influence.

The set of values from each test method were compared to the set of measured values using regression analysis. The correlation coefficients for  $R_{abs}$  are very high in each case. In testing the precision of the weather station model,  $K_{abs}$  is extremely well estimated. The  $L_{abs}$  are exposed as the greatest source of error in the weather station model.

A perfect correlation would have a slope ( $\beta$ ) equal

to 1 and a zero offset (y intercept). The Student  $t$ -test was performed on the data, testing for the null hypothesis that the slope is not equal to 0. The  $t$ -test indicates that the null hypothesis is true, the slope is not equal to 0. In each case, the null hypothesis was proven at the confidence interval of 99.9995%. This result is sufficiently significant to warrant no further testing of the data at this stage.

These two analyses have also been conducted on the sets of short wave and long wave radiation values estimated by the weather station model and measured by the radiometers. All findings are listed in Table 7. The  $R_{abs}$  estimated by the CRT assures that a very strong positive relationship exists between the measured values and the values as estimated by the CRT and weather station model.

### Summary and conclusions

This research, undertaken to measure and estimate radiation in complex outdoor environments under clear sky conditions, has proven very successful. Given the effect of wind and air temperature, the cylindrical radiation thermometer (CRT) and the model developed by Brown and Gillespie (1986) accurately measure the radiation available for absorption by an upright cylindrical body. At this stage, few if any designers are using human thermal comfort models to design outdoor environments as the data were either inaccessible or interpreted incorrectly (Cherkezoff 1987). In the past, if human thermal comfort was a consideration in the decision matrix, it was an intuitive 'guestimate' on the part of the individual designer, immeasurable and incomparable. The CRT then, provides access to data quickly and conveniently and the model provides an estimate within a 10% tolerance. This tolerance is acceptable as the levels of human thermal comfort are identified within ranges of radiation absorbed. Limiting these initial investigations to clear sky conditions meant one variable fewer to estimate, hence one fewer possible source of error. Further study is underway to test the CRT in a wider range of sun/cloud conditions and seasons.

The weather station model, founded on the principles of micrometeorological physics produced accurate estimates within 10% in all twelve test cases. The equations used in this model were taken from the literature and are recognized as valid models but are perhaps not as

**Table 7.** Test results of regression analysis and Student  $t$ -test

$x$ variable: $y$ variable	Correlation coefficient $r$	Offset & std.error. $\alpha \pm \text{SE}$	Slope & std.error, $\beta \pm \text{SE}$	H: $\beta \downarrow 0$ $H_o: \beta \uparrow 0$ $t^a$
Measured $R_{abs}$ : CRT $R_{abs}$	0.9499	$92.80 \pm 19.84$	$0.8116 \pm 0.0845$	9.607
Measured $R_{abs}$ : WS $R_{abs}$	0.9529	$126.20 \pm 16.82$	$0.7118 \pm 0.0717$	9.933
Measured $K_{abs}$ : WS $K_{abs}$	0.9865	$20.16 \pm 10.00$	$0.8565 \pm 0.0449$	19.075
Measured $L_{abs}$ : WS $L_{abs}$	0.8654	$109.83 \pm 15.72$	$0.6644 \pm 1216$	5.462

<sup>a</sup> The hypothesis (H) in the Student  $t$ -test is for  $\beta$  (slope) being 0.  $\beta = 0$ . Test proves to 0.995 confidence level, that the (H)ypothesis is false. The last column indicates strength that a relationship exists between Measure  $R_{abs}$  and the  $R_{abs}/L_{abs}/K_{abs}$  indicated by WS + CRT

flexible in all situations tested here. Similarly, usefulness of the model will rely on the ability of the investigator to make accurate estimates of site conditions. This becomes more difficult as the site increases in complexity. Though the sensitivity tests proved no single element is particularly sensitive, tables listing the albedo and average transmissivity of common elements in the landscape and techniques, such as suggested by Watson and Johnson (1988), for estimating sky view factor may provide more accurate modelling.

The human thermal comfort energy budget models allow a designer to consider micrometeorological parameters in the analysis, design and evaluation processes. Using a CRT and a minimum of time and microclimate expertise, a designer can identify variations in radiation load and map these as part of the inventory to use in

the analysis of the site. Before the final design plans are confirmed, the site is modelled using data from the nearest weather station and parameters of the site as designed, to understand and modify the microclimates that have been created on the site. With the advent of powerful computer workstations and advanced graphic software, these models could be adapted to simulate "3D images" of the radiant environment and map various comfort zones.

The original intent of this research was to describe radiation absorbed by a vertical cylinder in complex outdoor environments. Some plants and animals have also been considered as analogous to cylinders. The models and instruments used in this study can be readily adapted to studies of plant and animal survival in complex outdoor environments.

#### Appendix I. Inputs to weather station model

	Measured weather station values		Estimated values				
	Short wave $K_t$	Solar elevation	Sky view factor	Diffuse %	Albedo of objects in sky hemisphere <sup>a</sup>	Temperature of objects and ground <sup>c</sup>	Full sun %
Manitoba maple	678	40.30	0.20	15	18	18.25	30
Silver maple	640	38.21	0.60	15	18	18.27	15
Catalpa	710	44.57	0.50	15	18	18.50	25
Spruce 1	837	50.41	0.60	10	16	6.59	15
Spruce 2	749	44.89	0.60	15	16	18.24	15
Willow 1	747	44.83	0.25	10	18	4.77	75
Willow 2	743	44.39	0.10	15	18	18.22	30
Cedar	699	43.15	0.60	15	16	18.17	15
Open field 1	908	53.64	1.0	10	n/a	n/a	100
Open field 2	664	43.37	1.0	15	n/a	n/a	100
Open field 3	611	35.45	1.0	15	n/a	n/a	100
Building	813	45.74	0.50	10	40 <sup>b</sup>	14.95	0

<sup>a</sup> Campbell (1977) lists albedo of a deciduous woodland as 0.18 and a coniferous woodland as 0.16

<sup>b</sup> Dark buff brick is listed in Lam (1986) with an albedo of 0.40

<sup>c</sup> All objects in the test locations were assumed to be at air temperature

#### Appendix II. Equations of the weather station model

$$R_{abs} = K_{abs} + L_{abs} \quad (1)$$

$$K_{abs} = [(F + G + H) * (1 - A_o)] * (1 - A_c) \quad (2)$$

where:

$$F = K_{bvc} * t \quad (3)$$

$$G = K_d * SVF \quad (4)$$

$$H = K_d * (1 - SVF) * A_o \quad (5)$$

and:

$$K_{bvc} = \text{short wave beam incident on a vertical cylinder (in W/m}^2\text{)}$$

$$= [(K_t - K_d) * \tan(90 - \text{solar elevation})] / \pi \quad (6)$$

$$L_{abs} = [0.5 (N + P) + 0.5 (Q + S)] a \quad (7)$$

where:

$$N = L_s * SVF \quad (8)$$

$$P = L_{os} * (1 - SVF) \quad (9)$$

$$Q = L_g * P_g \quad (10)$$

$$S = L_{og} * (1 - P_{go}) \quad (11)$$

$$a = \text{estimated absorptivity of cylinder (0.95)}$$

and:

$$L_s = \text{Swinbank's formula for estimating long wave radiation under clear skies conditions (in W/m}^2\text{)}$$

$$= e [(\sigma 9.35 * 10^{-6}) T_a^6] \quad (12)$$

where:  $T_a$  = temperature of the air at 1.5 m (K)

$$e = \text{estimated emissivity of natural objects, } e = 0.95 \text{ (Campbell 1977)}$$

$$\sigma = \text{Stephan-Boltzmann equation } = 5.67 * 10^{-8} \quad (13)$$

$$SVF = \text{sky view factor: estimated proportion of the sky hemisphere unobstructed by tree/other objects}$$

$$L_{os} = \text{long wave radiation from object(s) in the sky hemisphere}$$

$$= e (\sigma T_o^4) \quad (14)$$

where:  $T_o$  = temperature of object (K)

$$L_g = \text{long wave radiation from the ground surface}$$

$$= e (\sigma T_g^4) \quad (15)$$

where:  $T_g$  = temperature of the ground (K)

$$P_g = \text{proportion of the ground of equal temperature}$$

## Appendix II. (continued)

$L_{og}$  = long wave radiation emitted from object(s) in the ground hemisphere  
 $= e (\sigma T_{og}^4)$   
 where:  $T_{og}$  = temperature of object(s) in the ground hemisphere (K)

(16)

$t$  = estimated proportion of incident radiation transmitted by natural object/material,  $t=0.95$  (Campbell 1977)

$K_d$  = estimated diffuse short wave radiation (in  $W/m^2$ )

$SVF$  = sky view factor: estimated proportion of the sky hemisphere unobstructed by tree/other object

$A_o$  = albedo of the object in the sky hemisphere

$K_l$  = short wave radiation in the open as measured by the Li-cor radiometer (in  $W/m^2$ )

$A_c$  = albedo of the painted cylinder surface is 0.37.

$K_l$  = 747 solar elevation = 44.83

$K_d$  = 10% (74.7) tan of (90-44.83) = 1.00595

$K_{bvc}$  = (747-74.7)\*1.00595/ $\pi$  = 215.27

$F$ : 215.27\*0.95 = 204.51

$G$ : 74.7\*0.25 = 18.68

$P_{og}$  = proportion of ground hemisphere occupied by the object(s)  
 $= (1 - P_g)$ .

(17)

$R_{abs}$  for the willow 1 test location are calculated using these equations with all radiation values in  $W/m^2$

$H$ : 74.7\*(1-0.25)\*0.18 = 10.08

$K_{abs}$  = (204.51 + 18.68 + 10.08)\*  
 0.82\*0.63 = 120.50

$T_a$  = 278K Assumption:

$T_s$  and  $T_o$  are also 278K

$L_s$  = 0.95 [(5.67\*10<sup>-8</sup>) (9.35\*10<sup>-6</sup>) (278)<sup>6</sup>] = 231.7

$N$ : 231.7\*0.25 = 57.9

$P$ : 338.65\*0.75 = 253.99

$Q$ : 338.65\*100338.65

$S$ : 338.65\*0 = 0

$L_{abs}$  = [0.5 (57.9 + 253.99) + 0.5 (338.65 + 0)] 0.95

$L_{abs}$  = 309.01

\* \* \*

$K_{abs} + L_{abs} = R_{abs}$

121 + 309 = 430

(slight discrepancies in these numbers are due to rounding to two decimal places only.)

Appendix III. Sensitivity tests<sup>1</sup> of weather station model inputs (using willow 1 inputs as example)

$K_l$	Solar elevation	Diffuse % of	SVF %	Object albedo	Temperature Object & Ground	Full sun %	$R_{abs}$ by a cylinder	$R_{abs}$ %	Input %	% $R_{abs}$ : %Input <sup>2</sup>
747	44.83	10	75	18	4.77	75	430			
475	44.83	10	75	18	4.77	75	386	-10	- 36	1:4
1015	44.83	10	75	18	4.77	75	472	+10	+ 36	1:4
747	60.00	10	75	18	4.77	75	386	-10	+ 34	1:3
747	35.00	10	75	18	4.77	75	472	+10	- 22	1:2
747	44.83	0.1	75	18	4.77	75	411	- 5	- 99	1:20
747	44.83	34	75	18	4.77	75	473	+10	+ 240	1:24
747	44.83	10	0.1	18	4.77	75	425	- 1	- 99	1:99
747	44.83	10	100	18	4.77	75	430	0	+1000	n/a
747	44.83	10	75	0.1	4.77	75	423	- 2	- 99	1:50
747	44.83	10	75	100	4.77	75	458	+ 7	+ 456	1:65
747	44.83	10	75	18	26.50	75	472	+10	+ 455	1:46
747	44.83	10	75	18	-25.00	75	386	-10	- 624	1:62
747	44.83	10	75	18	4.77	43	386	-10	- 47	1:47
747	44.83	10	75	18	4.77	100	463	+ 8	+ 33	1:4

<sup>1</sup> The first line of values in the chart are those measured and estimated for the willow test location. Each input was then altered to produce a 10% change in  $R_{abs}$  of the cylinder

<sup>2</sup> Ratio shows the percentage change to input value required to produce one percentage change in  $R_{abs}$

## References

- Brown RD (1985) Estimation of remote microclimates from weather station data with applications to landscape architecture. University of Guelph, Ontario, Canada
- Brown RD, Gillespie T (1986) Estimating outdoor thermal comfort using a cylindrical radiation thermometer and an energy budget model. Int J Biometeorol 30:43-52
- Campbell GS (1977) An introduction to environmental physics. Springer, Berlin Heidelberg New York
- Cherkezoff LE (1988) Testing of traditional systems and design of a method for including microclimatology in landscape design. University of Guelph, Ontario, Canada
- de Freitas CR (1985) Assessment of human bioclimate based on thermal response. Int J Biometeorol 29:97-119
- Lam W (1986) Sunlighting as formgiver for architecture. Van Nostrand Reinhold, New York
- Watson ID, Johnson GT (1988) Estimating person view-factors from fish-eye lens photographs. Int J Biometeorol 32:123-128